Morphological changes in the conjunctiva, episclera and sclera following short-term miniscleral contact lens wear in rigid lens neophytes

Author

Alonso-Caneiro, David, Vincent, Stephen J, Collins, Michael J

Published

2016

Journal Title

Contact Lens and Anterior Eye

Version

Accepted Manuscript (AM)

DOI

10.1016/j.clae.2015.06.008

Morphological changes in the conjunctiva, episclera and sclera following short-term miniscleral contact lens wear in rigid lens neophytes

David Alonso-Caneiro PhD

Stephen J Vincent PhD

Michael J Collins PhD

Corresponding author: David Alonso-Caneiro

Affiliation for all authors:

Contact Lens and Visual Optics Laboratory, School of Optometry and Vision Science

Queensland University of Technology

Address for correspondence:

Contact Lens and Visual Optics Laboratory, School of Optometry and Vision Science

Queensland University of Technology

Room B556, O Block, Victoria Park Road, Kelvin Grove 4059

Brisbane, Queensland, Australia

Phone: 617 3138 5717, Fax: 617 3138 5880

Word count: 5409 (excluding abstract, legends and references),

Number of Figures: 4

Number of Tables: 4

Email: d.alonsocaneiro@qut.edu.au

Abstract

Purpose: To quantify the influence of short-term wear of miniscleral contact lenses on the morphology of the corneo-scleral limbus, the conjunctiva, episclera and sclera.

Methods: OCT of the anterior eye were captured before, immediately following 3 hours of wear and then 3 hours after removal of a miniscleral contact lens for 10 young (27 ± 5 years), healthy participants (neophyte rigid lens wearers). The region of analysis encompassed 1 mm anterior to 3.5 mm posterior to the scleral spur. Natural diurnal variations in thickness were measured on a separate day and compensated in subsequent analyses.

Results: Following 3 hours of lens wear, statistically significant tissue thinning was observed across all quadrants, with a mean decrease in thickness of -24.1 ± 3.6 µm ($p<0.001$), which diminished, but did not return to baseline 3 hours after lens removal (-16.9 ± 1.9 µm, $p<0.001$). The largest tissue compression was observed in the superior quadrant (-49.9 ± 8.5 µm, $p<0.01$) and in the annular zone 1.5 mm from the scleral spur (-48.2 ± 5.7 µm), corresponding to the approximate edge of the lens landing zone. Compression of the conjunctiva/episclera accounted for about 70% of the changes.

Conclusions: Optimal fitting miniscleral contact lenses worn for three hours resulted in significant tissue compression in young healthy eyes, with the greatest thinning observed superiorly, potentially due to the additional force of the eyelid, with a partial recovery of compression 3 hours after lens removal. Most of the morphological changes occur in the conjunctiva/episclera layers.

Keywords: miniscleral contact lens, scleral thickness, corneo-scleral limbus

Introduction

Miniscleral contact lenses are manufactured from rigid gas permeable (RGP) polymers with an overall diameter of 14 to 17 mm [1, 2] and are of particular benefit to patients with corneal conditions including corneal ectasia (e.g. keratoconus), a history of penetrating keratoplasty, surface irregularity or contact lens intolerance associated with severe dry eye [3-5]. The lenses are designed to vault the cornea and limbus, with the haptic landing zone bearing entirely on the sclera and overlying ocular tissues [6]. The corneal vaulting results in the formation of a tear fluid reservoir (the post-lens tear layer) between the lens and the cornea, which can lead to optical, biomechanical and physiological advantages for the underlying cornea compared to other forms of contact lenses [7-10].

The distance between the posterior surface of the contact lens and the anterior surface of the cornea (i.e. the apical clearance) depends on the corneal geometry (primarily the corneal sagittal depth) and the lens design, and is routinely evaluated as part of the fitting procedure. The amount of apical corneal clearance is known to change over time, as the lens “settles” into the eye. The reduction in apical clearance during lens wear has been documented in various studies using both miniscleral and full scleral lens designs [11-14], with the majority of lens settling occurring within the first three to four hours following insertion [13]. This change in apical clearance following initial lens insertion may potentially be associated with tissue compression in the region of lens bearing (i.e. the landing zone of the lens).

Caroline and Andre [11] reported an average reduction in apical clearance of 96 µm (range 70 to 180 µm) following eight hours of lens wear for a 16.5 mm diameter miniscleral lens in 15 subjects with normal corneas. Using a similar lens diameter, Mountford [14] found the average lens settling after one month of lens wear to be 146 µm (range 106 to 186 µm) for a large cohort of 392 patients with various corneal conditions and lens designs. Michaud [12] also evaluated scleral lens settling in 23 subjects after a 6 hour period of wear for a 14.3 mm diameter lens and observed a mean decrease in apical clearance of 75 µm. More recently,

Kauffman and colleagues [13] reported on the lens settling for three different lens designs, which included two miniscleral (14.3 mm and 15.8 mm) and a full scleral design (18.2 mm), over an eight hour period for seven subjects with normal corneas. The magnitude of lens settling varied with each design, ranging from 88 to 133 µm. The reported changes in corneal clearance follow an exponential decay, with the majority of change occurring within the first 2 hours of lens wear and no significant differences (i.e. a plateau in corneal clearance) approximately 4 hours after lens insertion [13].

While the decrease in apical lens clearance over time is commonly observed in clinical practice, no study has measured the changes in the morphology of the ocular tissues surrounding the landing zone of scleral lenses. In this study, we used spectral domain optical coherence tomography to assess the short-term effect of 3 hours of miniscleral contact lens wear on the morphology of the corneo-scleral limbus, the conjunctiva/episclera and sclera and their recovery over the subsequent 3 hours. Image analysis methods were developed to allow repeated quantitative measurements at the same location on the ocular surface.

Methods

Participants were recruited from the staff and students of the Queensland University of Technology (QUT) Faculty of Health in Brisbane, Australia. Approval from the University Human Research Ethics Committee was obtained before commencement of the study, and subjects gave written informed consent to participate. All subjects were treated in accordance with the declaration of Helsinki.

The study participants included 10 young, healthy adult subjects (6 females, 4 males) between 21 and 33 years (mean ± SD age: 27 ± 5 years) with best corrected visual acuity of 0.00 logMAR or better. Prior to commencement of the study, all subjects were screened to exclude those with any contraindications to contact lens wear (i.e. significant tear film or anterior segment abnormalities). None of the subjects were previous rigid contact lens wearers and four of the subjects who were part-time soft contact lens wearers discontinued

lens wear for 24 hours prior to commencing the study. This should have allowed any substantial effects of soft lens wear on the morphology of the cornea and sclera to resolve [15]. Participants had no prior history of eye injury, surgery or current use of topical ocular medications.

Limbal and scleral imaging

The Spectralis optical coherence tomographer (OCT) with anterior segment module (Spectralis, Heidelberg Engineering, Heidelberg, Germany) was also used to obtained cross sectional images of the corneoscleral limbus, conjunctiva/episclera and sclera from four different quadrants (superior, inferior, nasal and temporal). This instrument uses a super luminescent diode of central wavelength 870 nm, which provides images with an axial resolution of 3.9 μm and transversal resolution of 14 μm, with a scanning speed of 40,000 A-scans per second. A high resolution volumetric scanning protocol was used (8.3 x 2.6 mm) consisting of 21 B-scans (each separated by 124 μm). The short wavelength of the instrument allows for high resolution imaging, however it does provide less imaging depth compared to longer wavelength systems. To compensate for this, images were obtained using the enhanced depth imaging (EDI) mode that optimises the posterior scleral interface. The instrument utilizes a confocal scanning laser ophthalmoscope (SLO) to automatically track the eye in real-time, and this function was active during the examination to achieve an average of 15 images per B-scan. A total of three volumetric scans were captured for each quadrant for each of the measurement sessions. Only images with a scan quality index of >20dB were included in the analysis (mean value 39.3 ± 3.9dB).

While the instrument can track the eye during image acquisition to allow for precise alignment and averaging of B-scans which reduces noise and improves contrast, the instrument's "auto-rescan" function, which automatically registers repeated scans taken at different times to the same location during acquisition, is only available for posterior segment imaging and not anterior segment imaging. Thus, during acquisition, care was taken to

position the volume scan in approximately the same limbal location (i.e. 3, 6, 9 and 12 o'clock) for all repeated measurements. Custom written software was developed to use the SLO image to accurately align OCT images between each measurement session for each participant and this procedure is described in the following section. The software was validated in terms of the observer's repeatability, showing that on average there was no difference in the selected B-scan between the repetitions.

The OCT instrument used in this study is limited by a maximum imaging depth of 1.9 mm. To optimise image quality, subjects maintained a fixed head position in the chin rest while looking peripherally to external LED fixation targets placed about 30° off-axis at different locations to facilitate the imaging of different scleral quadrants. This ensured that the measured region (i.e. the tissue surface) was quasi-perpendicular to the instrument, and minimised the depth to the posterior sclera, resulting in enhanced contrast across the horizontal scan.

Experimental procedure

The study protocol was conducted over three separate days; day one for general ophthalmic screening and miniscleral contact lens fitting and two additional days of data collection. On the second day, OCT diurnal measurements were taken without contact lens wear and on the third day the OCT measurements were taken before and after contact lens wear. Prior to the OCT measurements, corneal topography and thickness (Pentacam HR system, Oculus, Germany) were also captured at each measurement session to examine any corneal effects of lens wear and these changes have been reported elsewhere [16].

Initial baseline measurements were obtained in the morning (0 hours, session 1) and then repeated 3 hours (session 2) and 6 hours later (session 3). On the second day, the subject did not wear a contact lens and the natural diurnal variations of the combined conjunctiva/episcleral thickness and scleral thickness were recorded. On the third day, the subjects wore an optimal fitting miniscleral contact lens in their left eye only, with

measurements collected in the morning before the lens was inserted (0 hours, session 1), immediately after lens removal following 3 hours of wear (session 2) and finally 3 hours after lens removal (i.e. 6 hours after initial lens insertion) (session 3).

The timing of the measurement sessions on days two and three were matched for each participant to minimize any potential confounding influence due to diurnal variations in the morphology of the anterior eye [17] and were scheduled between 9:00-11:00 AM (session 1), 12:00-2:00 PM (session 2) and 3:00-5:00 PM (session 3). Between measurement sessions, participants were free to go about their daily activities, however, most remained in our laboratory engaged in computer based work or study. Measurements on day two (no lens wearing day) were conducted at least 12 hours after the initial contact lens fitting (on day 1) to minimise the influence of any ocular surface changes associated with the fitting process.

Following the removal of the contact lens on the third day (after three hours of lens wear), each participants left eye was re-examined using a slit lamp biomicroscope to assess the anterior eye. The Efron grading scale for contact lens complications [18] was used by the same examiner to quantify conjunctival fluorescein staining (inferior, superior, nasal and temporal) to the nearest 0.1 scale unit.

Contact lens assessment

The contact lenses used in this study were Irregular Corneal Design (ICD™ 16.5, Paragon Vision Sciences, USA) non-fenestrated miniscleral lenses made from hexafocon A material (Boston XO) with a Dk of 100 x 10^{-11} (cm^2/sec) (ml O_2/ml x mmHg), central thickness of 300 µm and an overall diameter of 16.5 mm. The optimal fitting contact lens was determined according to the manufacturers fitting guide. In brief, the initial lens fit was selected based on the participants corneal sagittal height measured over a 10 mm chord (along the steepest corneal meridian) using a videokeratoscope (E300, Medmont, Australia) which was then extrapolated to a 15 mm chord (i.e. the distance to the landing zone of the ICD lens) by

adding 2000 µm to the measured corneal sag over a 10 mm chord. The lens was inserted into the patients' left eye with preservative free saline and sodium fluorescein and assessed using a slit lamp biomicroscope. If an air bubble was present, the lens was removed and reinserted. The fluorescein pattern was assessed to ensure adequate central and limbal corneal clearance (i.e. no corneal bearing). If regions of corneal bearing were observed, the total sagittal depth of the lens (over a 15 mm chord) was increased incrementally by 100 µm and the fit reassessed until no corneal touch was evident. All lenses were inserted and removed by the same clinician (SJV). After an adequate initial fit was obtained, the lens was then allowed to settle for one hour, and was re-examined using the slit lamp. The final fluorescein pattern for all subjects showed central corneal clearance (sufficient to obscure visualisation of the pupil and iris features with sodium fluorescein), slight superior mid-peripheral to peripheral pseudo-bearing (an apparent area of bearing that disappeared on downward gaze) and sodium fluorescein "bleed" beyond the limbus onto the conjunctiva. Conjunctival blood vessels were examined under white light within the scleral landing zone to ensure there was no restriction or blanching of the vessels due to excessive peripheral seal off. The contact lens fit was assessed by the same examiner during the trial lens fitting (with sodium fluorescein) and on the day of lens wear (without sodium fluorescein) to ensure a well centred fit without any air bubbles. After one hour of lens settling (based on the manufacturers fitting guide), the corneal clearance (the distance between the back surface of the contact lens and the anterior corneal surface) was measured using the OCT centred on the corneal reflex. The group mean final central corneal clearance was 403 ± 204 µm. Alterations to the tangent curve of the limbal clearance zone or the edge lift of the scleral landing zone were not required to obtain an adequate fit, so during the experiment all participants wore the optimal fitting diagnostic trial lens which provided an initial central corneal clearance of at least approximately 300-400 µm.

Data analysis

Following data collection, the volumetric scans from the Spectralis OCT each containing one en-face SLO image and 21 B-scans, were exported and analysed using custom written software. Firstly, the volumetric scans were visually analysed to ensure that the quality and alignment of the OCT scans was acceptable and the best two of the three volume scans acquired for each session/quadrant were exported. Thus, for each measurement day, two SLO images per session/location were aligned with respect to the first measurement of session 1. To perform the alignment an experienced operator was presented with two images (the baseline and subsequent scans), and selected three anatomical landmarks per image (e.g. blood vessel bifurcations or intersections) in the en-face images representing common features between the images obtained at different times (Figure 1). Using these points, the amount of translation and rotation necessary to align the en-face images acquired at each subsequent measurement session with the baseline en-face image was determined. This allowed the thickness measurements within the OCT volume scan to be registered precisely to the same anatomical location of the anterior eye in each set of measurements. Of the two exported scans for each session/quadrant, the scan which displayed the least amount of rotation with respect to the baseline image was chosen for further analysis. The average absolute rotation for these scans selected for further analyses was 0.92 ± 0.89°.

Once the alignment between the en-face images was determined, the B-scan corresponding closest to the position of the central scan line of the baseline (session 1) measurement was identified in the aligned scans from sessions 2 and 3 taken later on the same day. This B-scan from each session was then analysed to segment the posterior scleral/posterior corneal boundary, the anterior scleral and anterior conjunctival/anterior corneal epithelium boundary. An initial automatic segmentation procedure was used to extract these two boundaries, after which one experienced observer, masked to the measurement session and day, assessed the integrity of the automated segmentation of the anterior conjunctiva and posterior sclera, and manually corrected any segmentation errors. The surface junction of the episclera and sclera was manually segmented, which was identified based upon the tissue appearance

and the presence of the episcleral blood vessels [19]. The masked observer then manually selected a vertical reference line to mark the position of the scleral spur in each OCT image [20]. This line was used as the reference location from which the thickness was averaged over 0.5 mm width segments. The analysis included two segments located anterior to the scleral spur (1 mm in total) that is referred to as the corneo-scleral (CS1 and CS2) regions and seven segments posterior to the scleral spur (3.5 mm in total) that we refer to as the scleral (S1 to S7) regions (Figure 2).

Using custom written software, the mean tissue thickness (anterior conjunctiva to posterior sclera) in each quadrant (nasal, temporal, superior, and inferior) and segments (CS1 to S7) were determined for each participant. In the corneo-scleral segments anterior to the scleral spur, the anterior tissue surface was either the conjunctiva or corneal epithelium surface. For locations posterior to the scleral spur, the anterior tissue surface was the conjunctival surface. The conjunctival/episleral thickness was only measured for the region posterior to the scleral spur, since the anterior zone encompassed the peripheral edge of the cornea [19].

The thickness data obtained on day 2, without contact lens wear, were then used to calculate the normal diurnal change in tissue thicknesses at each afternoon measurement time point (sessions 2 and 3) relative to the morning measurement (session 1). The same approach was then used to examine the influence of short-term miniscleral contact lens wear upon the tissue thickness profile. The mean session 1 (day 3) data (prior to lens insertion) was subtracted from both the session 2 (day 3) mean data (following lens removal) and also the session 3 (day 3) data (following 3 hours recovery) for each participant. To eliminate the potential confounding influence of diurnal variations, the normal diurnal changes calculated from the day 2 baseline data were also subtracted to generate ‘difference’ data (the change in tissue thickness immediately following lens removal and 3 hours after lens removal) which represents the changes due only to lens wear. All analyses presented refer to these data that have been corrected for normal diurnal variations in the tissue thickness. The diurnal

change averaged across all quadrants was small and less than 2 μm of thinning during the measurement day, without miniscleral lens wear.

Prior to statistical analyses, the Kolmogorov-Smirnov test confirmed that the data did not depart significantly from a normal distribution (all $p > 0.05$). To examine the statistical significance of changes due to short term miniscleral contact lens wear, a repeated measures analysis of variance (ANOVA) was used with quadrant (temporal, nasal, superior, inferior) and location with respect to the scleral spur (CS1, CS2, S1 to S7) as within-subject factors for the analysis of change in thickness. Degrees of freedom were adjusted using Greenhouse-Geisser correction to prevent any type 1 errors, where violation of the sphericity assumption occurred. Bonferroni adjusted post-hoc pair-wise comparisons were carried out for individual comparisons. A regression analysis was carried out to estimate the association between the magnitude of conjunctival and total tissue compression. All statistical analyses were conducted with SPSS (version 21.0) statistical software. P-values less than 0.05 were considered statistically significant. Descriptive statistics are reported as the mean and standard error.

Results

Regional tissue thickness

Table 1 presents the group mean total (sclera and conjunctiva/episclera combined) tissue thickness and standard error for the different locations and measurement quadrants before the insertion of the contact lens (session 1) (an average of session 1 on days 2 and 3). Repeated measures ANOVA revealed highly significant variations in baseline tissue thickness associated with both quadrant and location ($p<0.001$). Considering the nine locations in which the cross-sectional image was divided, the thickest location was the corneal/scleral limbus region (CS2, 812 ± 13 μm), while the thinnest location was 2 mm posterior to the scleral spur (S4, 708 ± 17 μm). Overall, the inferior quadrant was significantly thicker (815 ± 19 μm, $p<0.0001$) than all other quadrants (nasal 703 ± 16 μm,

temporal 727 ± 13 μm, superior 706 ± 21 μm), which were not statistically significantly different from each other ($p>0.05$).

Table 2 presents the group mean conjunctival/episcleral thickness for the different locations and measurement quadrants before the insertion of the contact lens (session 1) (an average of session 1 on days 2 and 3). Repeated measures ANOVA showed no significant variations in baseline conjunctival/episcleral thickness associated with either quadrant and/or location ($p>0.05$). The variation in conjunctival/episcleral thickness across the measured locations and quadrants was small (222 to 278 μm).

Regional thickness changes following contact lens wear

Figure 3 displays the group mean total tissue thickness change in locations anterior and posterior to the scleral spur, both immediately following and three hours after lens removal, relative to pre-lens wear measurements. Each subplot represents a region (temporal, nasal, superior, inferior), while each x-axis division represents a location relative to the scleral spur (CS1, CS2, S1 to S7) and the blue and red bars denote the time after lens removal (immediately following and three hours later). Figure 4 shows an example of the morphological change for two representative quadrants.

Statistically significant thinning was observed in the total thickness following three hours of lens wear with a mean decrease in thickness of -24.1 ± 3.6 μm (averaged over all regions and locations, $p<0.001$). This tissue compression diminished three hours after lens removal (-16.9 ± 1.9 μm), but was still significantly thinner relative to baseline ($p<0.001$). There was no correlation between the mean baseline total tissue thickness and the mean level of tissue compression, immediately following lens removal averaged across all regions ($r=0.20$, $p=0.50$). The association between the apical clearance of the lens and the magnitude of change in total tissue thickness immediately following lens removal was examined, which revealed a weak positive correlation when averaged across all regions examined, but did not reach statistical significance ($r=0.43$, $p=0.21$).

Table 3 presents the group mean total thickness change immediately following lens removal and after the three hour recovery period for each quadrant (averaged across all locations). Thinning was observed across all quadrants, with the superior region showing the largest change (-49.9 ± 8.5 µm, $p<0.01$), followed by the temporal quadrant (-19.8 ± 5.2 µm, $p<0.05$). Changes in the total tissue thickness for the nasal and inferior quadrants were on average less than 15 µm and did not reach statistical significance. Three hours after lens removal, the inferior total thickness had returned to near baseline levels (-3.8 ± 5.0 µm change, $p>0.05$), however the superior and temporal regions continued to show small but statistically significant ($p<0.05$) tissue compression (Table 3).

Table 4 presents the group mean thickness change both anterior and posterior to the scleral spur, and for the locations posterior to the scleral spur, also the change in individual layers of the tissue including the group mean conjunctival/episcleral change and the scleral change, immediately following lens removal and after the three hour recovery period for each location (averaged across all quadrants). For both time points, the locations within 3 mm posterior to the scleral spur (locations S1 to S6) showed statistically significant changes, with the greatest tissue compression observed at S3 (1.5 mm posterior to the scleral spur) immediately after lens removal (-48.2 ± 5.7 µm). Examining the change in each of the individual layers, the mean scleral thinning was substantially smaller (-4.9 µm) than the change in the conjunctiva/episclera (-19 µm). None of the scleral changes reached statistically significant values, while the conjunctival/episcleral were statically significant for the locations S1 to S6.

For all scleral locations (S1-S7) and regions (superior, inferior, nasal and temporal), the maximum compression values for the total thickness reached values (up to 48 µm) which correspond to 12% of the total tissue thickness, while for the conjunctiva/episclera it was approximately 30% of its thickness, and the scleral compression was below 2% of its total thickness. Linear regression revealed a positive association between the total thickness changes and the conjunctival/episcleral thickness changes ($p<0.001$; $R^2=0.637$, $\beta = 0.798$;

95% CI: 0.683 to 1.03), which indicates that most of the changes occurred at the conjunctival level.

Fluorescein staining

Trace levels of conjunctival fluorescein staining were observed following lens wear. Immediately after lens removal the mean grade of conjunctival staining was; 0.3 ± 0.1 inferiorly, 0.3 ± 0.2 superiorly, 0.3 ± 0.2 nasally and 0.3 ± 0.1 temporally. Conjunctival staining values less than grade 1.0 are considered clinically insignificant and do not require intervention [18].

Discussion

The reduction in apical clearance of miniscleral lenses over time is a well-established clinical phenomenon [13]. Examination of the changes within layers of the region posterior to the scleral spur revealed that the majority of tissue compression occurs in the conjunctiva/episclera, which accounted for approximately 70% of the total tissue compression, with less compression occurring in the underlying scleral layer. This is most likely because the underlying scleral tissue contains a dense network of collagen fibrils [21] which produces a more rigid biomechanical structure than the conjunctival/episcleral layers [22], which results in greater compression of the superficial tissue.

Following 3 hours of miniscleral lens wear, significant tissue compression was observed in the superior and temporal quadrants (averaged across all locations) and locations 1 to 3 mm posterior to the scleral spur (averaged across all quadrants). The magnitude of tissue compression was greatest superiorly, which may be the result of additional pressure applied by the superior eyelid on the contact lens [23]. While the location of the lower eyelid margin during primary gaze is typically near the lower limbus, the upper eyelid margin is typically positioned 2 to 3 mm below the superior limbus [24]. The potential toricity of the sclera, which could result in an uneven distribution of the load for a back surface spherical design,

like the one used in this experiment, may also be contribute to uneven tissue compression across quadrants.

The greatest mean total tissue change across all locations was observed between 1 to 2 mm posterior to the scleral spur, near to where the miniscleral lens landed on the ocular surface. If we consider an average corneal diameter (white-to-white) of 11.7 mm [25] and the landing zone (15 mm) and total diameter (16.5 mm) of the lenses used in this study, the lens should contact the sclera between 1.65 and 2.4 mm from the limbus (assuming no significant lens decentration, which was not measured in this study), and this matches well with the location of the greatest tissue compression that was observed. The findings in this paper are confined to one specific miniscleral lens design (with a 16.5 mm diameter). Larger diameter scleral lenses which land in a different anatomical region of the anterior segment (further from the limbus), will most likely result in a different profile of tissue compression. For example, Tenon's capsule, which is inseparable from the subconjunctival tissue and underlying episclera, becomes thicker about 3 mm from the limbus [26]. This tissue is thought to play an important role during larger scleral lens wear [27] and potentially influences compression of the tissue.

The scleral lens fit and settling characteristics may also be influenced by scleral topography (typically non-rotationally symmetric and flatter nasally compared to temporally [28]) and the position of the extraocular muscle insertion points (5.5 mm and ~7.0 mm from the nasal and temporal limbus respectively [29]). These factors have particular significance for larger scleral lenses (18.0 to 25.0 mm diameters), which may require a haptic back surface toric or quadrant specific designs (within the haptic/landing zone) to optimise the fit. While haptic back surface toric lens designs have been reported to improve lens comfort and increase wearing time, in this short-term study, a spherical back surface lens design was used for all participants, since there were no clinical indications that a modified lens design was required (e.g. localised regions of pressure resulting in conjunctival blanching, vessel impingement or significant fluorescein staining).

Three hours following lens removal, a residual thinning of the total baseline thickness was observed. The recovery of the tissue thickness differed between quadrants, with the inferior quadrant that showed the least thinning, returning to near baseline thickness values for all locations. The superior quadrant showed a reduction in tissue compression, although most locations posterior to the scleral spur remained statistically significantly different from the baseline thickness values. This trend was also observed for the nasal and temporal quadrants for the majority of the locations from 1 mm posterior to the scleral spur.

Baseline (pre-contact lens wear) measurements of conjunctival/episcleral thickness (mean 248 ± 15 μm) did not vary significantly with location, in agreement with previous OCT studies [19, 30]. However, the baseline measurements of total tissue thickness revealed significant variations that were quadrant and location specific. Overall, the inferior total tissue thickness was significantly thicker (mean 815 ± 10 μm) compared to the three other quadrants (nasal 703 ± 9 μm, temporal 727 ± 19 μm, superior 706 ± 10 μm). Other studies using time domain OCT [31] and magnetic resonance imaging [32] to obtain cross-sectional images of the sclera, have also reported that the total tissue thickness is greatest inferiorly. Patel [31] also observed that the sclera tends to be thicker closer to the scleral spur/limbus and remains relatively constant in thickness up to 2 mm and 3 mm posteriorly.

Given that this study examined ocular changes only after short-term wear (3 hours), a longer wearing time, similar to those observed during routine lens wear (i.e. 8 hours or more), is likely to result in larger magnitudes of tissue compression. However, a recent study by Kauffman [13] reporting on the dynamics of scleral lens settling, suggests that the majority of settling occurs within the first 4 hours of wear. Additionally, the biomechanical properties of the sclera have been shown to change with age [33, 34], race [33] and refractive error [35] and this could play a role in the dynamics of miniscleral lens settling. Thus, longer term studies including a wider range of healthy as well as eyes that would benefit optically or therapeutically from rigid contact lenses, are required to better understand the influence of extended periods of miniscleral lens wear on the conjunctival/episcleral and scleral

morphology. Although a significant correlation was not observed between central corneal clearance and the magnitude of tissue compression, it is likely that regional interactions between the lens design and the resulting tear layer between the contact lens and anterior eye topography (i.e. scleral topography/toricity) will influence the compression of the scleral tissue. Future studies considering different contact lenses design (i.e. haptic back surface torics vs. spherical designs) may help to provide further evidence of this effect. Similarly, a more detailed characterization of the post lens tear layer across the entire anterior segment [36], instead of the single apical corneal clearance captured in this study, is needed to better understand the influence corneal clearance and the potential role that this layer plays on the compression of the tissue in the landing zone. The variation in central corneal clearance between subjects may be a source of bias in the results, but also allowed us to investigate the association between the initial corneal clearance and the magnitude of tissue compression. While corneal clearance was not measured using OCT at the limbus in this study, the fluorescein pattern was examined immediately following lens insertion and after one hour of settling, as per the manufacturers fitting guide, and none of our participants exhibited regions of central or peripheral corneal touch which required refitting with an altered miniscleral lens design.

A further limitation of this study was the need to remove the miniscleral contact lens to obtain accurate measurements of tissue compression. As noted by a number of studies [37, 38], a contact lens in-situ produces an artefact in the OCT image, which may result in an overestimation of tissue compression [38]. Images taken with the contact lens in-situ should provide more realistic estimates of tissue morphology and the dynamic interaction between the lens and ocular tissues, however methods to automatically compensate for the artefacts introduced by the contact lens as well as refractive indexes for the different layers of contact lens and tissue are needed [39]. It would also be preferable to independently analyse the relative tissue compression in the conjunctival and episcleral tissues, however the current depth resolution of the OCT scan makes this challenging.

Previously, we investigated the influence of soft contact lens wear on the corneo-scleral limbus and the sclera [15] and found small (of up to 10 μm) but significant changes in the tissue morphology, which corresponded to less than 2% of total tissue compression. In this study we quantified the thickness changes of the cornea-scleral limbus, conjunctiva/episclera and sclera after short-term wear of miniscleral contact lenses, and found changes of up to 12% of the original total tissue thickness and up to 30% of the conjunctival/episcleral tissue thickness. However, given the limited number of reports of miniscleral contact lens complications [10], the long term clinical implications of these changes (if any) are yet to be determined. Interestingly conjunctival fluorescein staining, which is commonly used to assess the interaction between the contact lens edge and the ocular surface, was clinically insignificant following lens removal, despite the majority of tissue compression occurring at the level of the conjunctiva/episclera. Since miniscleral lenses do not move substantially with blinking (unlike smaller rigid lenses), the observed compression at the landing zone may not create substantial friction between the lens and the ocular surface.

Conclusion

Following short-term miniscleral contact lens wear, significant total tissue thinning was observed across the four quadrants of the anterior segment, with the greatest compression observed in the superior quadrant. This compression appears to occur primarily in the conjunctival/episcleral tissue. After the three hour recovery period following lens removal, the thickness values did not return to baseline values, except for the inferior quadrant. The association between the changes observed in the morphology of the tissue and other clinical findings is yet to be determined.

Acknowledgements

This study was partially funded by a QUT Institute of Health and Biomedical Innovation Vision Domain Development Grant. The authors acknowledge the assistance of Dr Alyra

Shaw during the early stages of the project as well as Emily Henry and Emily Woodman for assistance with the OCT image analysis.

References

[1] Vreugdenhil W, Geerards AJ, Vervae CJ. A new rigid gas-permeable semi-scleral contact lens for treatment of corneal surface disorders. Cont Lens Anterior Eye. 1998;21:85-8.
[2] Winkler T. Corneo-scleral rigid gas permeable contact lens prescribed following penetrating keratoplasty. Int Contact Lens Clin. 1998;25:86-8.
[3] Dalton K, Sorbara L. Fitting an MSD (mini scleral design) rigid contact lens in advanced keratoconus with INTACS. Cont Lens Anterior Eye. 2011;34:274-81.
[4] Ye P, Sun A, Weissman BA. Role of mini-scleral gas-permeable lenses in the treatment of corneal disorders. Eye Contact Lens. 2007;33:111-3.
[5] Sonsino J, Mathe DS. Central Vault in Dry Eye Patients Successfully Wearing Scleral Lens. Optom Vis Sci. 2013;90:e248-e51.
[6] van der Worp E, Bornman D, Ferreira DL, Faria-Ribeiro M, Garcia-Porta N, González-Meijome JM. Modern scleral contact lenses: a review. Cont Lens Anterior Eye. 2014;37:240-50.
[7] Visser ES, Visser R, van Lier HJ, Otten HM. Modern scleral lenses part I: clinical features. Eye Contact Lens. 2007;33:13-20.
[8] Michaud L, van der Worp E, Brazeau D, Warde R, Giasson CJ. Predicting estimates of oxygen transmissibility for scleral lenses. Cont Lens Anterior Eye. 2012;35:266-71.
[9] Ye P, Sun A, Weissman BA. Role of mini-scleral gas-permeable lenses in the treatment of corneal disorders. Eye & contact lens. 2007;33:111-3.
[10] Schornack MM. Scleral Lenses: A Literature Review. Eye contact lens. 2015;41:3-11.
[11] Caroline J P, Andre P A. Scleral lens settling. Contact Lens Spectrum. 2012;27:1.
[12] Michaud L. Variation of clearance with mini-scleral lenses. . Paper presented at the Global Specialty Lens Symposium, Las Vegas, NV, January 2014.
[13] Kauffman MJ, Gilmartin CA, Bennett ES, Bassi CJ. A Comparison of the Short-Term Settling of Three Scleral Lens Designs. Optom Vis Sci. 2014;91:1462-6.
[14] Mountford J. Scleral contact lens settling rates. 10th Congress of the Orthokeratology Society of Oceania (OSO), Queensland, Australia, July 2012. 2012.
[15] Alonso-Caneiro D, Shaw AJ, Collins MJ. Using optical coherence tomography to assess corneoscleral morphology after soft contact lens wear. Optom Vis Sci. 2012;89:1619-26.
[16] Vincent SJ, Alonso-Caneiro D, Collins MJ. Corneal changes following short-term miniscleral contact lens wear. Cont Lens Anterior Eye. 2014;37:461-8.
[17] Read SA, Collins MJ. Diurnal variation of corneal shape and thickness. Optometry and vision science : official publication of the American Academy of Optometry. 2009;86:170-80.
[18] Efron N. Grading scales for contact lens complications. Ophthal Physl Opt. 1998;18:182-6.
[19] Zhang X, Li Q, Liu B, Zhou H, Wang H, Zhang Z, et al. In vivo cross-sectional observation and thickness measurement of bulbar conjunctiva using optical coherence tomography. Invest Ophthalmol Vis Sci. 2011;52:7787-91.
[20] Seager FE, Wang J, Arora KS, Quigley HA. The effect of scleral spur identification methods on structural measurements by anterior segment optical coherence tomography. J Glaucoma. 2014;23:e29-e38.
[21] Watson PG, Young RD. Scleral structure, organisation and disease. A review. Exp Eye Res. 2004;78:609-23.
[22] Grant CA, Thomson NH, Savage MD, Woon HW, Greig D. Surface characterisation and biomechanical analysis of the sclera by atomic force microscopy. J Mech Behav Biomed. 2011;4:535-40.

[23] Shaw AJ, Collins MJ, Davis BA, Carney LG. Eyelid pressure and contact with the ocular surface. Invest Ophth Vis Sci. 2010;51:1911-7.
[24] Read SA, Collins MJ, Carney LG. The morphology of the palpebral fissure in different directions of vertical gaze. Optom Vis Sci. 2006;83:715-22.
[25] Rüfer F, Schröder A, Erb C. White-to-white corneal diameter: normal values in healthy humans obtained with the Orbscan II topography system. Cornea. 2005;24:259-61.
[26] Bergmanson JP. Clinical ocular anatomy and physiology: Texas Eye Research and Technology Center; 2011.
[27] van der Worp E. A Guide to scleral lens fitting. 2015.
[28] Van der Worp E, Graf T, Caroline P. Exploring beyond the corneal borders. Contact Lens Spectrum. 2010;6:26-32.
[29] Sevel D. The origins and insertions of the extraocular muscles: development, histologic features, and clinical significance. T Am Ophthal Soc. 1986;84:488.
[30] Zhang X, Li Q, Xiang M, Zou H, Liu B, Zhou H, et al. Bulbar conjunctival thickness measurements with optical coherence tomography in healthy Chinese subjects. Invest Ophthalmol Vis Sci. 2013;54:4705-9.
[31] Patel H. Biomechanical aspects of the anterior segment in human myopia (thesis): Aston University; 2011.
[32] Norman RE, Flanagan JG, Rausch SM, Sigal IA, Tertinegg I, Eilaghi A, et al. Dimensions of the human sclera: thickness measurement and regional changes with axial length. Exp Eye Res. 2010;90:277-84.
[33] Grytz R, Fazio MA, Libertiaux V, Bruno L, Gardiner SK, Girkin CA, et al. Age-and Race-related Differences in Human Scleral Material Properties. Invest Ophth Vis Sci. 2014;55:8163-72.
[34] Geraghty B, Jones SW, Rama P, Akhtar R, Elsheikh A. Age-related variations in the biomechanical properties of human sclera. J Mech Behav Biomed. 2012;16:181-91.
[35] Sergienko NM, Shargorogska I. The scleral rigidity of eyes with different refractions. Graef Arch Clin Exp. 2012;250:1009-12.
[36] Alonso-Caneiro D, Vincent SJ, Shaw AJ, Collins MJ. Scheimpflug imaging of the post lens tear film during contact lens wear. Proceedings of the VII European/1st World Meeting in Visual and Physiological Optics VPOptics 2014: Oficyna Wydawnicza Politechniki Wrocławskiej; 2014.
[37] Wolffsohn JS, Drew T, Dhallu S, Sheppard A, Hofmann GJ, Prince M. Impact of Soft Contact Lens Edge Design and Midperipheral Lens Shape on the Epithelium and Its Indentation With Lens Mobility. Invest Ophthalmol Vis Sci. 2013;54:6190-6.
[38] Sorbara L, Simpson TL, Maram J, Song ES, Bizheva K, Hutchings N. Optical edge effects create conjunctival indentation thickness artefacts. Ophthal Physl Opt. 2015.
[39] Westphal V, Rollins A, Radhakrishnan S, Izatt J. Correction of geometric and refractive image distortions in optical coherence tomography applying Fermat's principle. Optics Express. 2002;10:397-404.

Table 1. Group mean total thickness (mean ± SEM) (μm) for the different measurement quadrants and locations anterior to the scleral spur (CS1 and CS2) and posterior to the scleral spur (S1 to S7).

Location	Quadrant				
	Nasal	Temporal	Superior	Inferior	Mean
CS1 [1.0~0.5mm]	726 ± 9	791 ± 2	724 ± 9	783 ± 3	756 ± 2
CS2 [0.5~0.0mm]	761 ± 8	848 ± 2	773 ± 1	866 ± 6	812 ± 3
S1 [0.0~0.5mm]	722 ± 4	795 ± 5	747 ± 4	877 ± 0	785 ± 6
S2 [0.5~1.0mm]	663 ± 6	710 ± 5	701 ± 2	823 ± 1	724 ± 5
S3 [1.0~1.5mm]	667 ± 0	684 ± 5	690 ± 1	806 ± 1	712 ± 6
S4 [1.5~2.0mm]	680 ± 3	674 ± 4	685 ± 1	795 ± 3	708 ± 7
S5 [2.0~2.5mm]	695 ± 3	674 ± 4	680 ± 2	792 ± 3	710 ± 7
S6 [2.5~3.0mm]	704 ± 3	677 ± 5	677 ± 2	794 ± 3	713 ± 8
S7 [3.0~3.5mm]	712 ± 5	688 ± 7	678 ± 2	795 ± 3	719 ± 20
Mean	703 ± 16	727 ± 13	706 ± 21	815 ± 19	

Table 2. Group mean conjunctival/episcleral thickness (mean ± SEM) (μm) for the different measurement quadrants and locations posterior to the scleral spur.

Location	Quadrant				Mean
	Nasal	Temporal	Superior	Inferior	
S1 [0.0~0.5mm]	236 ± 15	222 ± 11	278 ± 11	271 ± 15	251 ± 8
S2 [0.5~1.0mm]	243 ± 14	255 ± 10	264 ± 11	272 ± 14	259 ± 7
S3 [1.0~1.5mm]	237 ± 14	266 ± 10	253 ± 12	266 ± 16	256 ± 7
S4 [1.5~2.0mm]	230 ± 15	260 ± 11	240 ± 14	248 ± 18	245 ± 8
S5 [2.0~2.5mm]	231 ± 17	247 ± 10	233 ± 16	239 ± 19	238 ± 9
S6 [2.5~3.0mm]	242 ± 18	236 ± 11	236 ± 18	241 ± 19	239 ± 10
S7 [3.0~3.5mm]	255 ± 20	230 ± 11	247 ± 20	254 ± 22	246 ± 12
Mean	239 ± 16	245 ± 9	250 ± 15	256 ± 17	

Table 3. Regional total tissue thickness change (compression) (mean ± SEM) (μm) immediately following lens removal and after the three hour recovery period for each quadrant.

	Thickness change (μm)	
Quadrant	**0h after removal**	**3h after removal**
Nasal	-12.8 ± 5.2	-21.2 ± 3.9**
Temporal	-19.8 ± 5.2*	-23.8 ± 4.5*
Superior	-49.9 ± 8.5**	-18.9 ± 5.4*
Inferior	-14.0 ± 7.2	-3.8 ± 5.0

Values where a pairwise comparison revealed a statistically significant change from baseline measurements (*$p<0.05$, ** $p<0.01$).

Table 4. Location specific total tissue thickness change (mean ± SEM) (μm) immediately following lens removal and after the three hour recovery period for each location.

	Thickness change (μm)					
	Total tissue		Conjunctiva/episclera		Sclera	
Location	0h after removal	3h after removal	0h after removal	3h after removal	0h after removal	3h after removal
CS1 [1.0~0.5mm]	6.9 ± 5.8	-13.9 ± 4.1*	-	-	-	-
CS2 [0.5~0.0mm]	-8.1± 6.4	-16.9 ± 4.1*	-	-	-	-
S1 [0.0~0.5mm]	-28.6 ± 7.6*	-28.5 ± 2.3*	-21.8 ± 8.5*	-19.8 ± 7.7*	-6.8 ± 7.3	-8.6 ± 7.2
S2 [0.5~1.0mm]	-43.8 ± 6.7*	-25.5 ± 2.1*	-38.1 ± 8.7*	-16.4 ± 6.7*	-5.6 ± 6.0	-9.0 ± 5.4
S3 [1.0~1.5mm]	-48.2 ± 5.7*	-19.7 ± 1.9*	-41.8 ± 7.5*	-14.8 ± 5.5*	-6.3 ± 5.9	-4.8 ± 4.3
S4 [1.5~2.0mm]	-40.0 ± 6.6*	-15.7 ± 3.5*	-37.2 ± 7.1*	-15.6 ± 4.6*	-2.8 ± 5.5	-0.1 ± 4.0
S5 [2.0~2.5mm]	-27.7 ± 6.1*	-12.9 ± 2.9*	-22.1 ± 5.9*	-10.9 ± 4.5*	-5.5 ± 4.8	-1.9 ± 4.5
S6 [2.5~3.0mm]	-17.4 ± 5.7*	-12.2 ± 2.1*	-13.3 ± 4.8*	-8.0 ± 6.5*	-4.1 ± 4.5	-4.1 ± 5.6
S7 [3.0~3.5mm]	-10.3 ± 4.8	-6.9 ± 2.0*	-4.3 ± 5.6	-4.1 ± 6.4	-5.9 ± 4.9	-2.7 ± 5.3

Values where a pairwise comparison revealed a statistically significant change from baseline measurements (*$p<0.05$). The negative values represent thinning. Thickness of the conjunctiva/episclera and sclera were not measured anterior to the scleral spur (CS1 and CS2).

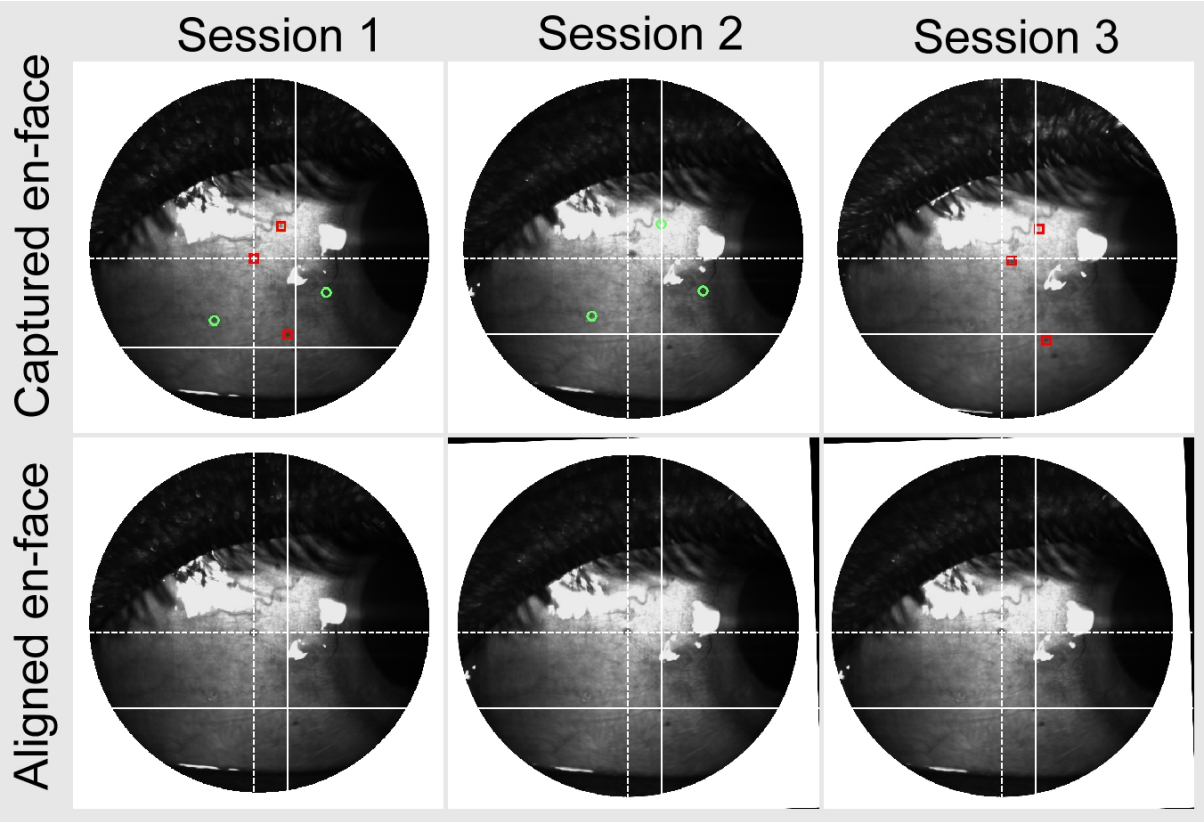

Figure 1. *Example of en-face SLO images for the same subject captured at different times during the measurement day (top row), session 1 to 3 respectively, and the equivalent aligned SLO images following adjustment (bottom row). Session 1 was pre-lens wear, session 2 was after 3 hours of lens wear and session 3 was 3 hours after lens removal. The three manually selected matching points per image represent common features between the baseline (session 1) and subsequent scans (sessions 2 and 3), with green points corresponding to sessions 1 & 2 and red points to sessions 1 & 3. Using these points, the amount of image translation and rotation necessary to align the en-face images acquired at each session with the baseline en-face image was determined. Dashed and solid cross lines mark the same position in each image, to appreciate the results of the alignment.*

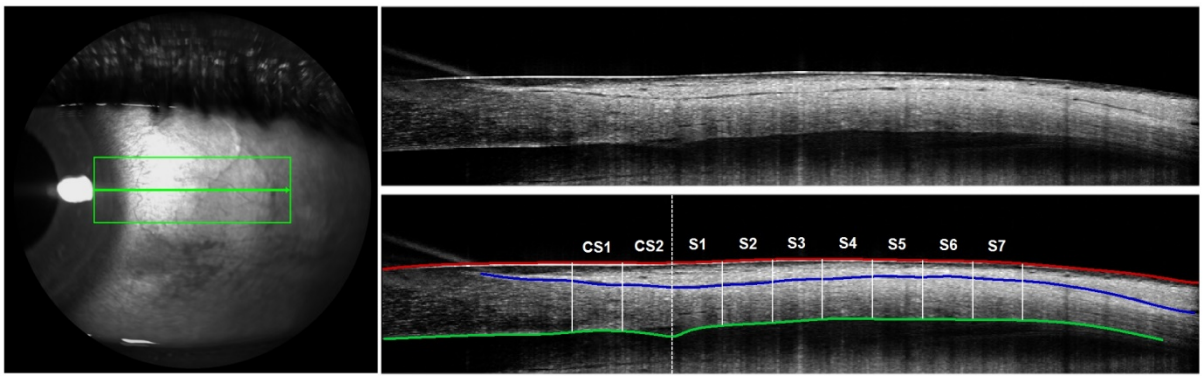

Figure 2. *Illustration of the scanning protocol used to image the anterior segment (left), and an example OCT image (right). Original (right-top) and segmented (right-bottom) B-scan with the three boundaries of interest (anterior conjunctiva [red line], anterior [blue line] and posterior sclera [green line]). The vertical dashed white line (marks the scleral spur) was used as the reference from which the scleral thickness was averaged over 0.5 mm length sections. Two locations were anterior to the scleral spur (CS1 and CS2, 1 mm in total) and seven were posterior to the scleral spur (S1 to S7, 3.5 mm in total).*

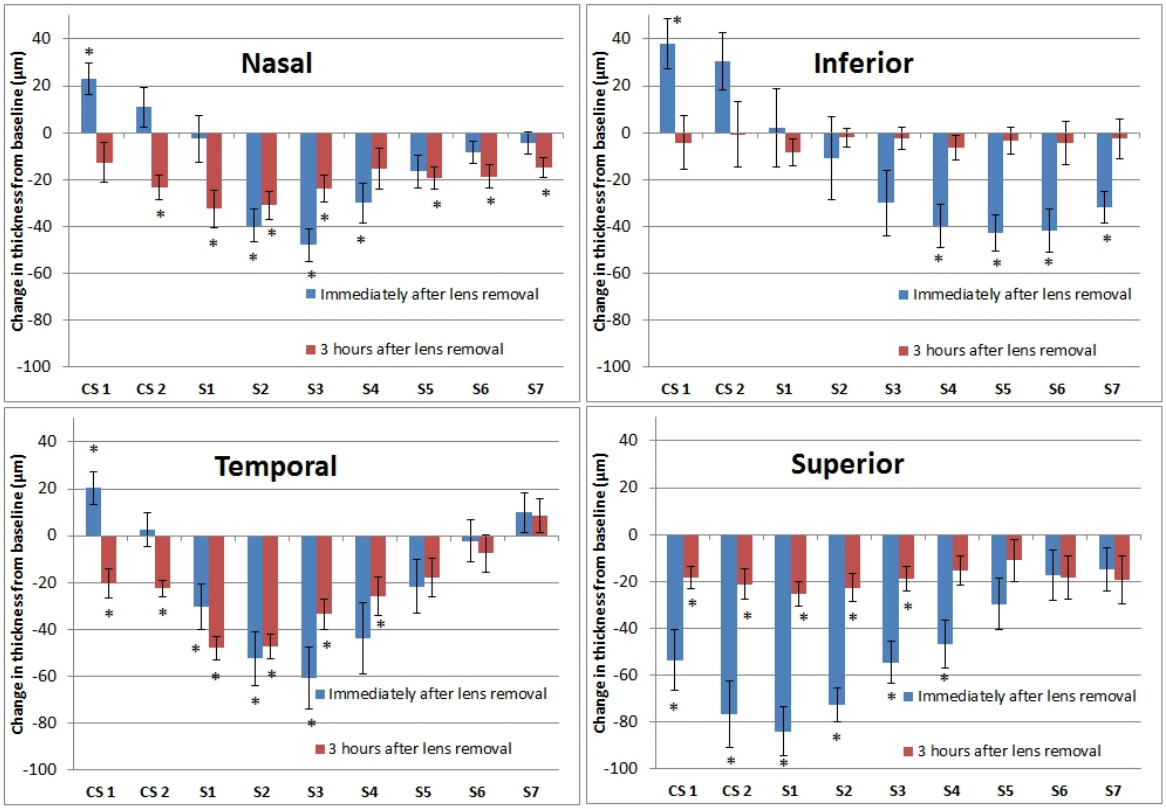

Figure 3. *The group mean total thickness change (mean ± SEM) (µm) immediately following lens removal (blue bars) and after the three hour recovery period (red bars) for the different regions and locations. Asterisk (*) indicates values where a pairwise comparison revealed a statistically significant change from baseline ($p<0.05$). The negative values represent thinning and positive values represent thickening.*

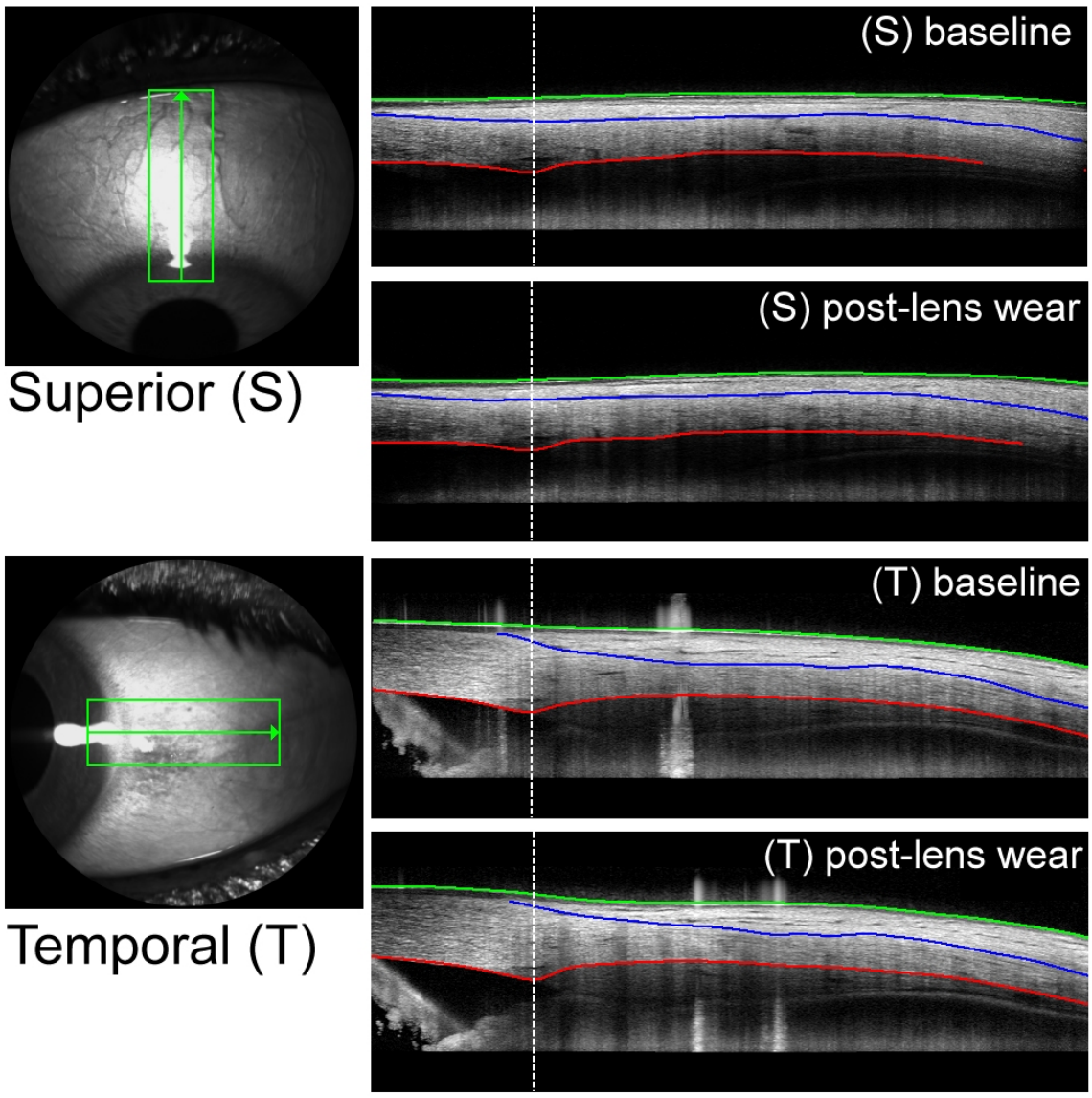

Figure 4. *Example of B-scans for the same subject taken at baseline (immediately before lens insertion) and the corresponding B-scan post-lens wear (immediately after 3 hours of lens wear) for two representative quadrants (S-superiror, T-temporal). Some of the thinning and morphology changes in the conjunctiva and episclera can be observed in the B-scans immediately after lens removal.*